$AgOC(CF_3)_3$: Synthesis and Applications of the First Donor-Free Silver(I) Alkoxide†

Andreas Reisinger, Nils Trapp, and Ingo Krossing*

Institut für Anorganische und Allgemeine Chemie, Albert Ludwigs Universität Freiburg, Albertstrasse 21, D-79104 Freiburg, Germany

Received November 14, 2006

The Li alkoxide $LiOR^F$ (**1**) ($R^F = C(CF_3)_3$) was quantitatively prepared by reacting stoichiometric amounts of LiH and HOR^F. Upon reaction of **1** with 1 equiv of $AgBF_4$, the first donor-free Ag(I) alkoxide $AgOR^F$ formed in 86% yield. The Ag alkoxide was then used for the preparation of trigonal bipyramidal $[(AgL)_3(OR^F)_2]^+$ cage cations (L = C_2H_4 (**3**), C_4H_8 (**4**)) stabilized by weakly coordinating $[Al(OR^F)_4]^-$ counterions. **1** to **4** were characterized by multinuclear NMR, IR, and Raman spectroscopy as well as by their single-crystal X-ray structures and additional quantum chemical calculations.

Introduction

Main group and transition metal alkoxides have a long history in chemistry *inter alia* owing to their applications in organometallic synthesis or as precursors for electronic or ceramic materials.[1] In the case of the group 11 metals, several of the homoleptic Cu(I) alkoxides have been tested in CVD processes and turned out to be very promising.[2] However, information on donor-free coinage metal alkoxides is still sparse and limited to Cu.[3−6] Of these Cu(I) alkoxides, only $CuOCR_3$ (R = CH_3 and C_6H_5) have been structurally characterized.[5,6] All these compounds are tetranuclear and form approximately square planar eight-membered rings in the solid state (Figure 1), unless donors such as CO, alkenes, or phosphines are supplied, which changes their structures to heterocubane-type aggregates[7,8] or dinuclear four-membered rings[6,8,9] depending on R and the donor molecule.

Even though the preparation of these copper(I) alkoxides turned out to work rather well,[4] no homologous compounds with Ag or Au have been reported, except one poorly characterized phosphine adduct.[3] However, Ag(I) alkoxides might, similar to the copper compounds, be versatile reagents in organometallic synthesis, e.g., the synthesis of new weakly coordinating anions that complement the known alkoxy aluminates of type $[Al(OR^F)_4]^-$ (R^F = fluorinated alkyl or aryl group).[10−13] These aluminates have been widely used in our group.[14,15] Silver alkoxides might be promising precursors for Ag CVD processes, since only a few volatile Ag compounds are currently known.[16] $AgOR^F$ could also be used to form a trigonal bipyramidal $[Ag_3(OR^F)_2]^+$ cage cation from Ag^+ and 2 $AgOR^F$. Such trinuclear group 10 or 11 metal complexes stabilized by bridging bidentate bis(diphenylphosphino)methane (dppm) or ethane (dppe) ligands and two capping μ^3 ligands X (Figure 2) are well known.[17] Such $[M_3X_2(dppm)_3]$ complexes are known for M = Ni,[18] Pd,[19] Pt,[20,21]

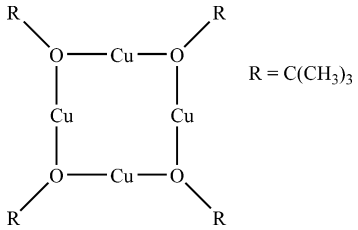

Figure 1. Schematic drawing of the square planar tetranuclear CuOR structure.

† Dedicated to Prof. H. Willner at the Bergische Universität in Wuppertal, Germany, on the occasion of his 60th birthday.

* Corresponding author. E-mail: krossing@uni-freiburg.de.

(1) Hubert-Pfalzgraf, L. G. *Coord. Chem. Rev.* **1998**, *178−180*, 967−997. Hubert-Pfalzgraf, L. G.; Guillon, H. *Appl. Organomet. Chem.* **1998**, *12*, 221−236. Veith, M.; Weidner, S.; Kunze, K.; Kaefer, D.; Hans, J.; Huch, V. *Coord. Chem. Rev.* **1994**, *137*, 297−322. Bradley, D. C. *Chem. Rev.* **1989**, *89*, 1317−22.

(2) Terry, K. W.; Lugmair, C. G.; Gantzel, P. K.; Tilley, T. D. *Chem. Mater.* **1996**, 8, 274−80. Drake, I. J.; Fujdala, K. L.; Baxamusa, S.; Bell, A. T.; Tilley, T. D. *J. Phys. Chem. B* **2004**, *108*, 18421−18434. Fujdala, K. L.; Drake, I. J.; Bell, A. T.; Tilley, T. D. *J. Am. Chem. Soc.* **2004**, *126*, 10864−10866. Jeffries, P. M.; Girolami, G. S. *Chem. Mater.* **1989**, *1*, 8−10.

(3) Schmidbaur, H.; Adlkofer, J.; Shiotani, A. *Chem. Ber.* **1972**, *105*, 3389−96.

(4) Tsuda, T.; Hashimoto, T.; Saegusa, T. *J. Am. Chem. Soc.* **1972**, *94*, 958−959.

(5) Greiser, T.; Weiss, E. *Chem. Ber.* ***1976***, *109*, 3142−3146. Hakansson, M.; Lopes, C.; Jagner, S. *Inorg. Chim. Acta* **2000**, *304*, 178−183.

(6) Lopes, C.; Hakansson, M.; Jagner, S. *Inorg. Chem.* **1997**, *36*, 3232−3236.

(7) Geerts, R. L.; Huffman, J. C.; Folting, K.; Lemmen, T. H.; Caulton, K. G. *J. Am. Chem. Soc.* **1983**, *105*, 3503−3506. Hakansson, M.; Lopes, C.; Jagner, S. *Organometallics* **1998**, *17*, 210−215.

(8) Lopes, C.; Hakansson, M.; Jagner, S. *Inorg. Chim. Acta* **1997**, *254*, 361−366.

(9) Lemmen, T. H.; Goeden, G. V.; Huffman, J. C.; Geerts, R. L.; Caulton, K. G. *Inorg. Chem.* **1990**, *29*, 3680−5.

(10) Ivanova, S. M.; Nolan, B. G.; Kobayashi, Y.; Miller, S. M.; Anderson, O. P.; Strauss, S. H. *Chem. Eur. J.* **2001**, *7*, 503−510. Krossing, I.; Reisinger, A. *Inorganic Chemistry in Focus II*; 2005; pp 65−87. Krossing, I.; Reisinger, A. *Coord. Chem. Rev.* **2006**, *250*, 2721−2744.

(11) Krossing, I.; Brands, H.; Feuerhake, R.; Koenig, S. *J. Fluor. Chem.* **2001**, *112*, 83−90.

(12) Krossing, I. *Chem. Eur. J.* **2001**, *7*, 490−502.

(13) Krossing, I.; Reisinger, A. *Eur. J. Inorg. Chem.* **2005**, *10*, 1979−1989.

(14) Krossing, I.; Raabe, I. *Angew. Chem., Int. Ed.* **2001**, *40*, 4406−4409. Krossing, I. *J. Am. Chem. Soc.* **2001**, *123*, 4603−4604. Krossing, I.; Van Wüllen, L. *Chem. Eur. J.* **2002**, *8*, 700−711. Krossing, I. *J. Chem. Soc., Dalton Trans.* **2002**, *4*, 500−512. Cameron, T. S.; Decken, A.; Dionne, I.; Fang, M.; Krossing, I.; Passmore, J. *Chem.−Eur. J.* **2002**, *8*, 3386−3401. Krossing, I.; Bihlmeier, A.; Raabe, I.; Trapp, N. *Angew. Chem., Int. Ed.* **2003**, *42*, 1531−1534.

(15) Krossing, I.; Reisinger, A. *Angew. Chem., Int. Ed.* **2003**, *42*, 5725−5728.

(16) Edwards, D. A.; Harker, R. M.; Mahon, M. F.; Molloy, K. C. *J. Chem. Soc., Dalton Trans.* **1997**, 3509−3513. Purdy, A. P.; George, C. F. *ACS Symp. Ser.* **1994**, *555*, 405−20.

(17) Burrows, A. D.; Mingos, D. M. P. *Coord. Chem. Rev.* **1996**, *154*, 19−69.

10.1021/om061046p CCC: $37.00
Publication on Web 03/10/2007

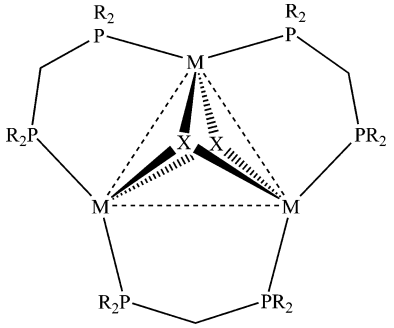

Figure 2. Schematic drawing of the trinuclear $[M_3X_2(dppm)_3]$ framework.

Cu,[22−25] and Ag.[26−28] Group 11 metal complexes with X = F,[20,29] Cl,[26,27] Br,[26,30,31] I,[26,30,32] NCO,[26] CNR,[25] OH, OR,[24] SR,[24] RC_2,[23,28,33] and others are known. Recently also hydride was intercalated into the Cu_3 triangle.[34]

However, no group 10 or 11 metal structure *including* the trigonal bipyramidal framework but *without* the chelating diphosphine ligands has been reported. In fact, this leads to the question of whether these compounds have considerable metal−metal interactions and would be stable without the chelating ligands or whether they are just held together by the diphosphine ligands.

(18) Maekawa, M.; Munakata, M.; Kuroda-Sowa, T.; Hachiya, K. *Inorg. Chim. Acta* **1995**, *233*, 1−4. Manojlovic-Muir, L.; Muri, K. W.; Mirza, H. A.; Puddephatt, R. J. *Organometallics* **1992**, *11*, 3440−3444.

(19) Manojlovic-Muir, L.; Muir, K. W.; Lloyd, B. R.; Puddephatt, R. J. *J. Chem. Soc., Chem. Commun.* **1983**, 1336−1337. Manojlovic-Muir, L.; Muir, K. W.; Lloyd, B. R.; Puddephatt, R. J. *J. Chem. Soc., Chem. Commun.* **1985**, 536−537. Lloyd, B. R.; Manojlovic-Muir, L.; Muir, K. W.; Puddephatt, R. J. *Organometallics* **1993**, *12*, 1231−1237. Rashidi, M.; Kristof, E.; Vittal, J. J.; Puddephatt, R. *J. Inorg. Chem.* **1994**, *33*, 1497−1501.

(20) Lloyd, B. R.; Puddephatt, R. J. *J. Am. Chem. Soc.* **1985**, *107*, 7785−7786.

(21) Ferguson, G.; Lloyd, B. R.; Manojlovic-Muir, L.; Muir, K. W.; Puddephatt, R. J. *Inorg. Chem.* **1986**, *25*, 4190−4197. Ferguson, G.; Lloyd, B. R.; Puddephatt, R. J. *Organometallics* **1986**, *5*, 344−348. Douglas, G.; Jennings, M. C.; Manojlovic-Muir, L.; Muir, K. W.; Puddephatt, R. J. *J. Chem. Soc., Chem. Commun.* **1989**, 159−161. Bradford, A. M.; Douglas, G.; Manojlovic-Muir, L.; Muir, K. W.; Puddephatt, R. J. *Organometallics* **1990**, *9*, 409−416. Bradford, A. M.; Kristof, E.; Rashidi, M.; Yang, D.-S.; Payne, N. C.; Puddephatt, R. J. *Inorg. Chem.* **1994**, *33*, 2355−63.

(22) Bera, J. K.; Nethaji, M.; Samuelson, A. G. *Inorg. Chem.* **1999**, *38*, 218−228.

(23) Diez, J.; Gamasa, M. P.; Gimeno, J.; Aguirre, A.; Garcia-Granda, S. *Organometallics* **1991**, *10*, 380−382. Diez, J.; Gamasa, M. P.; Gimeno, J.; Lastra, E.; Aguirre, A.; Garcia-Granda, S. *Organometallics* **1993**, *12*, 2213−2220.

(24) Diez, J.; Gamasa, M. P.; Gimeno, J. *Polyhedron* **1995**, *14*, 741−745.

(25) Diez, J.; Gamasa, M. P.; Gimeno, J.; Aguirre, A.; Garcia-Granda, S. *Organometallics* **1997**, *16*, 3684−3689.

(26) Di Nicola, C.; Effendy; Fazaroh, F.; Pettinari, C.; Skelton, B. W.; Somers, N.; White, A. H. *Inorg. Chim. Acta* **2005**, *358*, 720−734.

(27) Zhang, P.; Zhang, Y.; Zheng, L.; Yang, H.; Zhang, Q. *Xiamen Daxue Xuebao, Ziran Kexueban* **1990**, *29*, 549−52.

(28) Wang, C.-F.; Peng, S.-M.; Chan, C.-K.; Che, C.-M. *Polyhedron* **1996**, *15*, 1853−1858.

(29) Straub, B. F.; Rominger, F.; Hofmann, P. *Inorg. Chem.* **2000**, *39*, 2113−2119. Straub, B. F.; Rominger, F.; Hofmann, P. *Inorg. Chem.* **2000**, *39*, 2113−2119.

(30) Morgenstern, D. A.; Ferrence, G. M.; Washington, J.; Henderson, J. I.; Rosenhein, L.; Heise, J. D.; Fanwick, P. E.; Kubiak, C. P. *J. Am. Chem. Soc.* **1996**, *118*, 2198−2207.

(31) Yang, R.-N.; Sun, Y.-A.; Hu, X.-Y.; Jin, D.-M. *Chin. J. Chem.* **1999**, *17*, 284−292.

(32) Zhou, W.-B.; Dong, Z.-C.; Song, J.-L.; Zeng, H.-Y.; Cao, R.; Guo, G.-C.; Huang, J.-S.; Li, J. *J. Cluster Sci.* **2002**, *13*, 119−136.

(33) Yam, V. W.-W.; Lee, W.-K.; Cheung, K.-K.; Crystall, B.; Phillips, D. *J. Chem. Soc., Dalton Trans.* **1996**, 3283−3287.

(34) Mao, Z.; Huang, J.-S.; Che, C.-M.; Zhu, N.; Leung, S. K.-Y.; Zhou, Z.-Y. *J. Am. Chem. Soc.* **2005**, *127*, 4562−4563.

Table 1. Comparison of the ^{7}Li, ^{13}C, and ^{19}F NMR Shifts of 1 and 2 in CD_2Cl_2 with $NaOR^F$ [37] and DFT-Calculated Shifts (BP86/SV(P))

	$LiOR^F$, **1**		$AgOR^F$, **2**		$NaOR^F$
	exptl	calc[a]	exptl	calc[a]	
δ^7Li	−2.81 (s)				
δ^{13}C, $C(CF_3)_3$	83.1 (dez)	86.6	82.0 (dez)	83.7	
$^2J_{CF}$ [Hz]	28.1		26.9		
δ^{13}C, $C(CF_3)_3$	124.2 (q)	132.3	122.9 (q)	131.6	
$^1J_{CF}$ [Hz]	292.4		293.3		
δ^{19}F, $C(CF_3)_3$	−77.42 (s)	−80.5	−75.94 (s)	−81.9	−81.1

[a] The calculation of the NMR shifts has been carried out with optimized geometries of solvent-free tetrameric **1** (heterocubane structure; t symmetry) and **2** (ring structure; S_4 symmetry). Optimized geometries are deposited as Supporting Information.

Herein we report the synthesis and characterization of $AgOR^F$ ($R^F = C(CF_3)_3$) starting from the respective Li alkoxide. This is the first example of a structurally characterized donor-free Ag alkoxide. A preliminary account of one of the structures has already been given.[35] This Ag alkoxide has been used to form the first trigonal bipyramidal $[M_3X_2]^+$ cages free of chelating diphosphine ligands.

Results and Discussion

Synthesis. Initially, $[(AgC_2H_4)_3(OR)_2][Al(OR^F)_4]$ (**3**, in the following: $R^F = C(CF_3)_3$) was formed as a side product during the synthesis of $[Ag(C_2H_4)_3][Al(OR^F)_4]$.[15] However, the formation of **3** suggested the existence of a hitherto unknown donor-free silver(I) alkoxide. To our belief, the impurity that led to the formation of **3** was most probably a trace of LiH (in the bulk $LiAlH_4$), which reacted with the perfluorinated alcohol $HOC(CF_3)_3$ to give the respective Li alkoxide. In the following metathesis reaction with AgF the Li atom was replaced by Ag, similarly to the formation of the silver alkoxy aluminates. According to this scheme, we assessed a systematic approach to prepare a donor-free silver alkoxide and reproduce the synthesis of **3**.

Preparation of MOR^F (M = Li, Ag). $LiOR^F$ (**1**) was prepared according to the literature[36,37] from HOR^F in Et_2O (eq 1) as a colorless powder in 99% yield. From the THF solution, the Li alkoxide crystallized as a dimeric THF adduct (**1a**), whereas solvent-free tetrameric crystals were obtained by recrystallization from hot (∼80 °C) 1,2-difluorobenzene (**1b**).

$$LiH + HO{-}RF \xrightarrow[-\ H_2]{Et_2O} LiO{-}R^F \qquad (1)$$

The subsequent metathesis to the silver(I) alkoxide $AgOR^F$ (**2**) with AgX (X = F, BF_4) was done by mixing the two solids in the glovebox and suspending them in CH_2Cl_2 with exclusion of light (eq 2).

$$LiO\text{-}RF + AgX \xrightarrow[-\ LiX]{CH_2Cl_2} AgO{-}R^F \qquad (2)$$

$$X = F, BF_4$$

(35) Reisinger, A.; Himmel, D.; Krossing, I. *Angew. Chem. Int. Ed.* **2006**, *118*, 7153−7156.

(36) Samuels, J. A.; Lobkovsky, E. B.; Streib, W. E.; Folting, K.; Huffman, J. C.; Zwanziger, J. W.; Caulton, K. G. *J. Am. Chem. Soc.* **1993**, *115*, 5093−5094. Dear, R. E. A.; Fox, W. B.; Fredericks, R. J.; Gilbert, E. E.; Huggins, D. K. *Inorg. Chem.* **1970**, *9*, 2590−2591.

(37) Samuels, J. A.; Folting, K.; Huffman, J. C.; Caulton, K. G. *Chem. Mater.* **1995**, *7*, 929−35.

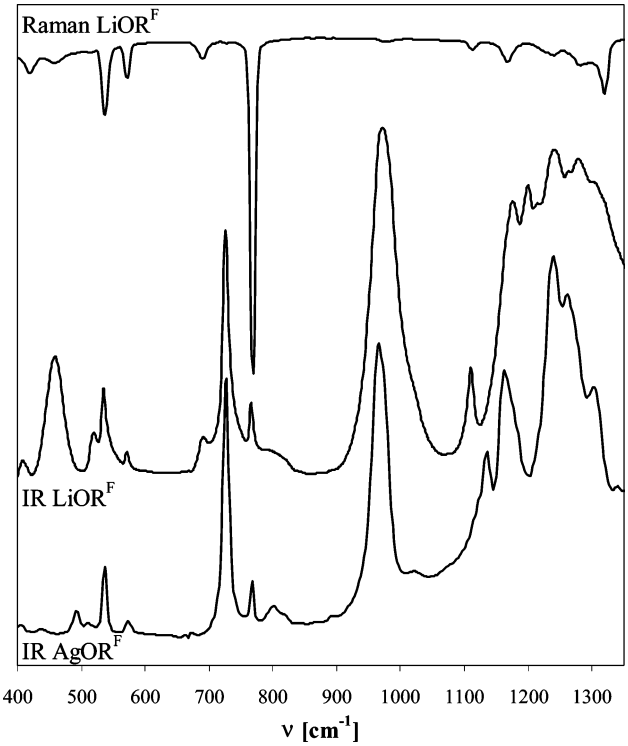

Figure 3. IR spectra of **1b** (middle) and **2b** (bottom) as well as the Raman spectrum of **1b** (top) in the range between 400 and 1350 cm^{-1}. The spectra have been scaled for comparison.

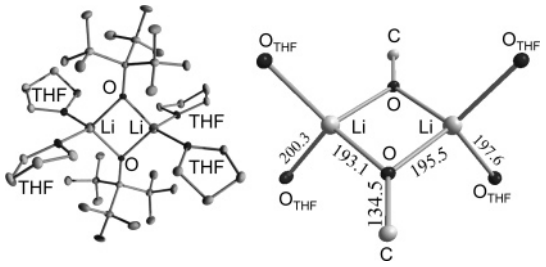

Figure 4. Section of the solid-state structure of **1a** (left) and detailed plot of the central square (right). Thermal ellipsoids were drawn at the 25% probability level. Hydrogen atoms of the ligand were added and isotropically refined. Bond lengths: Li−O 193.0(3) to 200.3(3) pm (av 196.6 pm); C−O 134.5(2) to 145.0(2) pm (av 142.7 pm); C−C 150.1(4) to 156.4(2) pm (av 153.3 pm); C−F 133.2(2) to 135.1(2) pm (av 134.3 pm).

Initially the reaction was attempted using the cheaper AgF. However, no reaction was observed at ambient temperature, and only upon treatment in an ultrasonic bath at 50 °C overnight did the suspension turn dark brown (Caution! CH_2Cl_2 has a bp of 40.6 °C). The solids were removed by filtration and a clear, colorless CH_2Cl_2 solution remained. After removal of the solvent 3−5 very small crystals remained that could be identified as the desired product **2**, but with a very poor yield. When the more soluble $AgBF_4$ was used instead, the suspension turned gray after stirring overnight at room temperature. After filtration large amounts of colorless crystals of a hemisolvate $AgOR^F \cdot (CH_2Cl_2)_{0.5}$ (**2a**) grew directly from the solution at −40 °C and were characterized by X-ray crystallography. Removal of the solvent led to a white powder (86% yield, isolated), which was characterized by NMR, IR, and Raman spectroscopy. Upon the loss of the intercalated CH_2Cl_2, dry **2** turned brown *in vacuo*, approximately within 1 h and probably due to the influence of light. However, dry and solid **2** is stable over several weeks in a −20 °C freezer and with exclusion of light. Furthermore, solvent-free **2** can be further purified by sublimation at 130 °C and 10^{-2} mbar.

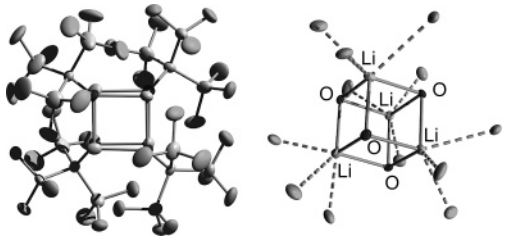

Figure 5. Section of the solid-state structure of **1b** (left) and detailed plot of the central cube including the Li−F contacts (right). Thermal ellipsoids were drawn at the 50% probability level. Bond lengths: Li−O 193.8(11) to 199.1(11) pm (av 196.1 pm); C−O 135.7(7) to 136.9(6) pm (av 136.2 pm); C−C 153.2(9) to 156.8(9) pm (av 155.2 pm); C−F 132.2(7) to 138.4(9) pm (av 134.6 pm).

Preparation of $[(AgL)_3(OR^F)_2][Al(OR^F)_4]$ (L = C_2H_4, i-C_4H_8). The successful formation of the silver alkoxide **2** provides a suitable reagent for a systematic approach to the accidentally synthesized trigonal bipyramidal cation in **3**. $[(AgL)_3(OR^F)_2][Al(OR^F)_4]$ (L = C_2H_4 (**3**), *i*-C_4H_8 (**4**)) were prepared from $Ag[Al(OR^F)_4]$ and 2 equiv of **2**, which were mixed in the glovebox and dissolved in CH_2Cl_2 in the presence of stoichiometric amounts of L (eq 3). Large, colorless, block-shaped crystals of **3** and **4** grew directly from the cooled (−20 °C) solution.

$$Ag[Al(OR^F)_4] + 2\ AgOR^F + 3\ L \xrightarrow[R^F = C(CF_3)_3,\ L = C_2H_4,\ i\text{-}C_4H_8]{CH_2Cl_2} [(AgL)_3(OR^F)_2][Al(OR^F)_4] \quad (3)$$

Interestingly the presence of a soft donor such as C_2H_4 or C_4H_8 is crucial for the successful synthesis of the trigonal bipyramidal cation. All attempts to form this compound with only CH_2Cl_2 failed and led to crystallization of the less soluble, compared to the alkoxyaluminate, alkoxide hemisolvate **2a**.

By contrast, in the presence of a suitable ligand, the cage cation shows some stability: when crystals of **3** were dissolved in CH_3CN and ESI-mass spectra were recorded, the weaker C_2H_4 ligand is replaced instantaneously by acetonitrile, but the trigonal bipyramidal structure of the cation appears to remain intact in the gas phase. One CH_3CN ligand was lost upon ionization and the peak of $[Ag_3(CH_3CN)_n(OR^F)_2]^+$ ($n = 2$) was observed with 100% relative intensity. All other peaks with $n = 1$ (0.3%) and $[Ag_2(CH_3CN)_m(OR^F)]^+$ $m = 1$ (0.1%), 2 (0.2%) were minor.

Properties of 1 and 2. NMR Spectroscopy. The ^{13}C and ^{19}F NMR spectra of **1** and **2** in CD_2Cl_2 are very similar and show the expected signals of the perfluorinated ^{t}Bu group (Table 1).[12,13,37] In comparison to **1**, the ^{13}C signals of the silver alkoxide are shifted to lower frequencies ($\Delta\delta = -1.1$ ppm for the tertiary carbon and −1.3 ppm for the carbon of the CF_3 groups), whereas the ^{19}F signals are shifted to higher frequencies ($\Delta\delta = +1.5$ ppm). Although the DFT-calculated values show an offset of about 3 to 8 ppm, the general trends for the ^{13}C shifts hold, while the calculated shifts for the ^{19}F spectrum are inverted compared to the experiment.

The discrepancy between experimental and calculated shifts may possibly be explained with different structures of **1** and **2** in solution; for example, the polymer **2** may form a hypothetic

Table 2. Experimental IR and Raman Bands of 1b and 2b Compared to Calculated DFT Frequencies ((RI-)BP86/SV(P))[a]

$LiOR^F$ (**1b**)			$AgOR^F$ (**2b**)		
IR	calculated	Raman	IR	calculated	Raman
	92 (ia)	116 (5)		104 (ia)	108 (14)
	153 (w) + 182 (w)	167 (1)		149 (vw) + 180 (vw)	168 (5)
	200 (ia)	220 (13)		217 (vw)	220 (7)
	271 + 304 (mw)	309 (21)		288 (vw)	300 (16)
	316 (vw) + 337 (w)	329 (28)		311 (vw)	329 (35)
	346	344 (34)		388 (vw)	361 (9)
408 (w)	423 (mw)	419 (6)	405(w)	400 (vw)	
459 (ms)	463 (mw)	458 (4)	435 (vw)		
	497 (ia)		493 (mw)	479 (w)	493 (4)
520 (mw)			510 (vw)	500 (vw)	506 (4)
535 (m)	517 (mw)	537 (21)	537 (m)	520 (w)	539 (19)
571 (w)	552 (w)	571 (10)	573 (w)	558 (vw)	573 (5)
691 (w)	676 (w)	690 (5)		674 (ia)	680 (5)
726 (s)	707 (mw)	706 (1)	726 (ms)	708 (mw) + 712 (mw)	726 (4)
766 (m)	747 (w)	769 (100)	767 (m)	751 (w)	770 (100)
			801 (mw)		806 (4)
972 (vs)	962 (ms)	976 (1)	966 (vs)	962 (ms)	984 (9)
1110 (m)	1077 (w)	1113 (4)	1135 (m)	1091 (w)	1114 (7)
1176 (s)	1133 (w) + 1153 (mw)	1168 (7)	1163 (ms)	1146 (s) + 1155 (mw)	1165 (9)
1200 (s)	1186 (vw) + 1193 (vw)			1186 (mw) + 1198 (w)	
1240 (vs)	1231 (vs)	1240 (5)	1240 (vs)	1224 (vs)	1240 (4)
			1261 (s)		1262 (9)
1279 (s)	1253 (s)	1282 (8)		1256 (s)	1290 (9)
	1290 (w)	1320 (17)	1303 (ms)	1274 (s)	1315 (14)

[a] IR and Raman bands of **2b** at 2726, 2850, 2900, and 2947 cm^{-1} originate from traces of CH_2Cl_2 and, therefore, have been omitted.

$[(CH_2Cl_2)Ag(OR^F)]_2$ dimer (cf.: a similar structure has been observed for $[(CH_2Cl_2)AgOTeF_5]_2$).[38]

Vibrational Spectroscopy. The IR spectra of **1b** and **2b**, shown in Figure 3, exhibit the typical bands of a perfluorinated ^{t}BuO group in the range between 400 and 1320 cm^{-1}. They may easily be assigned by comparison to other compounds that contain these groups[12,13] as well as to the calculated vibrational frequencies as demonstrated in Table 2. The bands between 2727 and 2946 that were observed in both spectra were caused by traces of CH_2Cl_2.

Solid-State Structures. $LiOR^F$·2 THF (1a) and $LiOR^F$ (1b). Crystals of **1a** were obtained by crystallization from a concentrated THF solution of **1** (Figure 4). In the solid-state structure, 2 equiv of the alkoxide form a centrosymmetric almost square planar ring with Li−O bond distances of 193.1(3) and 195.5(4) pm (194.3 pm av). The O−Li−O angle is larger (93.69(15)°) than the Li−O−Li angle (86.31(15)°). The two remaining free coordination sites of the tetrahedrally coordinated lithium atoms are occupied by THF molecules with longer Li−O bond distances of 197.6(4) and 200.3(4) pm.

Thin, plate-shaped crystals of **1b** were obtained by recrystallization of solvent-free $LiOR^F$ from hot (80 °C) *o*-difluorobenzene. The asymmetric unit consists of four formula units, where Li and O form an almost ideal heterocubane cage (Figure 5, left) with an average Li−O bond distance of 196.1 pm (193.8−199.1 pm). The O−Li−O angles are slightly larger (90.5−93.1°, 91.6° av) than the Li−O−Li angles (87.4−90.0°, 88.4° av). The central cube is shielded by four perfluorinated ^{t}Bu groups, where one F atom of each CF_3 group forms an intramolecular Li−F contact (221.3 to 264.9 pm, 242.2 pm av; Figure 5 right). The corresponding C−F bond distances are elongated by 1.9 pm (av) compared to the other C−F bonds (135.9 vs 134.0 pm). The point group symmetry of the tetramer is approximately T and, therefore, the experimental structure fits very well with the global minimum of the calculations. The heterocubane-type structure and numerous M−F contacts are in very good agreement with other lithium[39] and the homologous sodium alkoxides.[36,37]

$AgOR^F$·0.5CH_2Cl_2 (2a) and $AgOR^F$ (2b). Large, colorless, block-shaped crystals of **2a** grew directly from the CH_2Cl_2 filtrate at −40 °C. Although Ag is coordinated by two O atoms, the asymmetric unit of **2a** does not consist of an eight-membered ring as in the known copper alkoxides[5,6] as well as the recently published silver silyl oxide $AgOSi(^iPr)_3$.[35] By contrast, the asymmetric unit consists of only one formula unit where Ag and O reside on special crystallographic positions. Application of the symmetry operations of the space group results in the formation of infinite helices built from Ag and O and aligned along the crystallographic 4_1 screw axis. The $C(CF_3)_3$ groups are oriented outward with regard to the 4_1 screw axis and, due to the symmetry operations, are also disordered by rotation of 60° around the O−C bond axis ("umbrella effect"). While the $C(CF_3)_3$ groups form a tight shell around the helices, there is still some interstice left inside, which is occupied by CH_2Cl_2 distributed over two positions, exactly 0.5 solvent molecule per formula unit. Weak Ag−Cl contacts at about 314 and 335 pm are formed (cf. $\sum$(van der Waals radii) = 350 pm, Figure 6).

Small, colorless, rectangular-shaped crystals of solvent-free **2b** grew during sublimation of **2** at 130 °C and 10^{-2} mbar. Unlike the rectangular ring structures observed for Cu[5,6] and $AgOSi^iPr_3$,[35] the alkoxide **2b** forms a one-dimensional polymeric structure built up from distorted eight-membered rings that are connected through rectangular four-membered rings (Figure 7).[35] The centers of both 8 rings are the $\bar{1}$ positions of the lattice. One of the Ag atoms is almost linearly coordinated (172.7(2)°) by two O atoms, while the other Ag atom is coordinated by three O atoms in between a T-shape and a trigonal planar arrangement (81.603(9)°, 124.1(1)°, and 152.302(6)°). Within the eight-membered rings the average Ag−O bonds (221.2 pm) are elongated by 13.3 pm compared to the siloxide $AgOSi^iPr_3$ (207.9 pm). However, the elongation is more pronounced for

(38) Strauss, S. H.; Noirot, M. D.; Anderson, O. P. *Inorg. Chem.* **1985**, *24*, 4307−4311.

(39) Boyle, T. J.; Pedrotty, D. M.; Alam, T. M.; Vick, S. C.; Rodriguez, M. A. *Inorg. Chem.* **2000**, *39*, 5133−5146. Boyle, T. J.; Alam, T. M.; Peters, K. P.; Rodriguez, M. A. *Inorg. Chem.* **2001**, *40*, 6281−6286. Thiele, K.; Goerls, H.; Seidel, W. Z. *Anorg. Allg. Chem.* **1998**, *624*, 1391−1392.

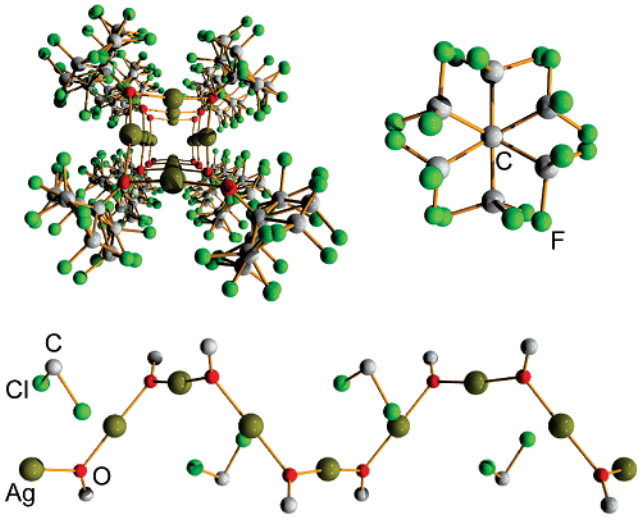

Figure 6. Sections of the solid-state structure of **2a**. Top left: View of one helix along the 4_1 screw axis; solvent molecules have been omitted for clarity. Top right: Disorder of one $C(CF_3)_3$ group caused by rotation of 60° around the C−O bond. Bottom: View perpendicular to the screw axis; CF_3 groups have been omitted for clarity. Only one possible orientation of CH_2Cl_2 is shown.

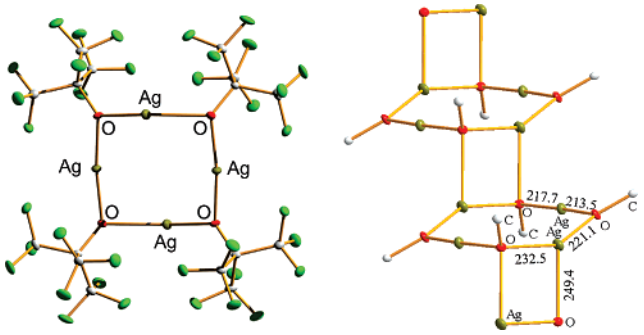

Figure 7. Sections of the solid-state structure of **2b**: eight-membered ring comprising two asymmetric units (left) and intermolecular Ag−O contacts of the individual rings (right, CF_3 groups have been omitted for clarity). Bond lengths: Ag−O 193.8-(11) to 199.1(11) pm (av 196.1 pm); C−O 135.7(7) to 136.9(6) pm (av 136.2 pm); C−C 153.2(9) to 156.8(9) pm (av 155.2 pm); C−F 132.2(7) to 138.4(9) pm (av 134.6 pm).

the T-shaped (221.1 and 232.5 pm) than for the linearly bonded silver (213.5 and 217.7 pm). This is accompanied by a long ring connecting the Ag−O bonds (249.4 pm), which are shorter than the Cu−O bonds of the related CuO^tBu structure (251.5 pm). This is in good agreement with the relatively high, compared to all other structures, distortion of the O−Ag−O and Ag−O−Ag angles (162.5° and 100.6°).

In agreement with an electrophilic silver ion that tends toward polymer formation, three Ag−F contacts per silver atom were observed in **2b** covering the range between 275.1 and 300.0 pm (av 288.6 pm, cf. Σ(van der waals radii) = 320 pm; Figure 8).

Properties of 3 and 4. NMR Spectroscopy. Signals of the ^{13}C, ^{19}F, and ^{27}Al NMR spectra of **3** and **4** that can be assigned to the anion $[Al(OR^F)_4]^-$ are detailed in the lower part of Table 4. They are similar to other salts of this anion and therefore are not discussed in detail.[11−13,15] Signals that were assigned to the cationic moieties of **3** and **4** are shown in the upper part. From the assignment of individual signals to the OR^F moieties of the anion and the cation it is clear that they are not involved in dynamic exchange on the time scale of NMR spectroscopy.

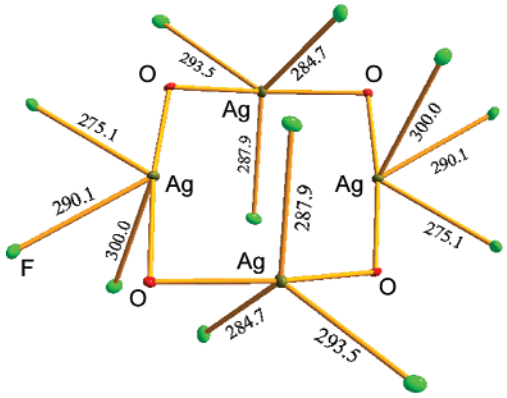

Figure 8. Ag−F contacts in the solid-state structure of **2b**.

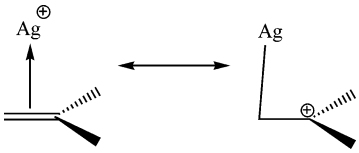

Figure 9. Likely $Ag(i\text{-}C_4H_8)^+$ resonance structures that account for the observed structure and chemical shifts in **4**.

Table 3. Selected Average Bond Distances and Angles of 1a, 1b, 2a, and 2b Compared to LiOPh and CuO^tBu (bond lengths in pm, angles in deg)

	$(LiOPh)_4$	**1a**	**1b**	$(CuO^tBu)_4$	**2a**	**2b**
d(M−O)	193.3	194.2	196.1	181.2	214.9(5)	221.2
d_{ion}(M−O)[a]	219			183	208	
d_2(M−O)[b]				251.5		249.4
d(O−C)	133.0	134.8	136.2	145.6	133.6(14)	138.4
w(O−M−O)	95.0	93.7	91.6	175.6	173.0(3)	162.5
w(M−O−M)	84.8	86.3	88.4	93.6	106.6(4)	100.6

[a] d_{ion} is the sum of the ionic radii of M^+ and O^{2-}. For M = Cu, Ag, the ionic radius for a coordination number of 4 has been employed.[40] [b] d_2 denotes the longer, ring-connecting M−O bond lengths.

Compared to free ethene, the proton signal of the ligand in **3** is shifted to higher frequencies ($\Delta\delta$ = +0.26 ppm), whereas the carbon signal is shifted to lower frequencies ($\Delta\delta$ = −11.1 ppm), which is in good agreement with the calculated shifts ($\Delta\delta$ = −11.6 ppm) and indicates the coordination to the Ag atom (Table 4). In the case of isobutene as a ligand, the two proton signals are both shifted to higher frequencies ($\Delta\delta$ = +0.09 and +0.39 ppm), which also holds for the ^{13}C signal of the methyl group ($\Delta\delta$ = +2.5 ppm) and is in agreement with the calculations ($\Delta\delta$ = 0.0, +0.4, and +1.6 ppm). In contrast, the coordination to the silver atom is no longer symmetric (see below, crystal structure). Thus the signal of the tighter bound CH_2 moiety is shifted to lower frequencies upon coordination ($\Delta\delta$ = −17.5 ppm), whereas the signal of the $C(CH_3)_2$ group is shifted to higher frequencies ($\Delta\delta$ = +17.0 ppm). This behavior is in very good agreement with the calculated values ($\Delta\delta$ = −18.7 and +17.4 ppm, Table 4). Both changes of the chemical shifts can be explained with the formation of a complex that points in the direction of the more stable carbocation, as one would expect according to Markovnikov's law and considering Ag^+ as a replacement for H^+.

In contrast to other alkene complexes,[41] no coupling to silver was observed in any of the ^1H and ^{13}C spectra of **3** and **4**. The

(40) Lide, D. R. *CRC Handbook of Chemistry and Physics*, 83rd ed.; CRC Press: Boca Raton, 2002.

(41) Thomaier, J.; Boulmaaz, S.; Schonberg, H.; Ruegger, H.; Currao, A.; Grützmacher, H.; Hillebrecht, H.; Pritzkow, H. *New J. Chem.* **1998**, *22*, 947−958.

Table 4. Comparison of the Experimental ^{1}H, ^{13}C, ^{19}F, and ^{27}Al NMR Shifts of 3 and 4 with Signals of the Free Alkene Ligands[42] and DFT-Calculated Shifts ((RI-)BP86/SV(P))[a]

	3		C_2H_4		**4**		C_4H_8	
	exptl	calc	exptl	calc	exptl	calc	exptl	calc
$\delta^{1}H$ (=H_2)	5.54	5.0	5.28	5.03	4.89	4.3	4.80	4.3
$\delta^{1}H$ (−CH_3)					2.09	1.8	1.70	1.4
$\delta^{13}C$ (=CH_2)	112.2	110.1	123.3	121.7	93.8	94.2	111.3	112.9
$\delta^{13}C$ (=$C(CH_3)_2$)					158.8	156.1	141.8	138.7
$\delta^{13}C$ (CH_3)					26.7	30.0	24.2	28.4
$\delta^{13}C$ ($C(CF_3)_3$)		83.1			82.0	83.8		
$\delta^{13}C$ (CF_3)	122.9	131.7			122.8	132.3		
$^{1}J_{CF}$ [Hz]	292.1				292.9			
$\delta^{19}F$ (CF_3)	−75.38	−79.0			−75.85	−79.5		
$\delta^{13}C$ ($C(CF_3)_3$)	-				79.7			
$\delta^{13}C$ (CF_3)	122.0				122.0			
$^{1}J_{CF}$ [Hz]	292.7				293.2			
$\delta^{19}F$ (CF_3)	−75.74				−75.74			
$\delta^{27}Al$	31.9				31.9			

[a] Cation signals are shown in the upper, anion signals in the lower part.

Table 5. Experimental IR and Raman Bands of the Cationic Part of 3 and 4 Compared to DFT-Calculated Frequencies (BP86/SV(P))[a]

$(AgC_2H_4)_3(OR)_2^+$ (**3**)			$(AgC_4H_8)_3(OR)_2^+$ (**4**)		
IR	calculated	Raman	IR	calculated	Raman
	409 (ia)	405 (10)		430 (mw)	431 (6)
501 (vw)	486 (vw)		501 (vw)	461 (w) + 490 (vw)	468 (16)
651 (w)	655 (vw)			653 (vw)	
671 (w)	674 (ia)	687 (5)	669 (w)	669 (vw)	
766 (mw)	748 (w)	770 (80)	765 (w)	749 (w) + 766 (vw)	770 (36)
902 (w)		903 (3)	930 (m)	916 (m)	934 (14)
	956 (s)	989 (11)		955 (s)	
1002 (m)	1002 (ia)	1007 (14)		993 (vw)	1004 (5)
1065 (w, sh)	1077 (w)		1075 (mw)	1056 (mw) + 1076 (w)	1061 (11)
	1283 (s)	1316 (100)		1360 (mw)	1378 (17)
				1370 (mw)	1393 (24)
				1402 (vw)	1407 (20)
1431 (w)	1414 (w)			1424 (mw)	1428 (17)
1454 (mw)			1459 (s)	1446 (mw)	1469 (6)
1578 (vw)	**1557 (vw)**	**1572 (44)**	**1586 (w)**	**1558 (mw)**	**1586 (27)**
		2757 (18)	2726 (w)		2745 (4)
2852 (ms)			2845 (s)		2837 (3)
2921 (m)		2909 (11)	2901 (s)	2944 (w)	2927 (39)
2954 (ms)		2937 (16)	2947 (s)	3024 (w)	
3009 (m)	3060 (vw)	3009 (59)		3044 (vw)	2993 (75)
3118 (w)	3144 (vw) + 3162 (vw)	3092 (11)	3177 (w)	3066 (w) + 3136 (vw)	3057 (5)

[a] The frequencies of the C=C stretches are shown in bold.

absence of a $^{1}J_{AgC}$ coupling can be explained with the nature of the respective ligands: ethene and methylpropene are fluxionally bound to the silver on the time scale of an NMR experiment. This can be underlined with the absence of an additional signal due to free dissolved ligand, even if an excess of olefin was used. Moreover, back-bonding is only minimal (cf. C=C stretching frequencies below) and the Ag−C bonding likely has only minimal s-character from the carbon side (σ-donation of π-electron density from the olefin to silver). Thus, the coupling of silver to carbon, which has to be transmitted by a Fermi contact mechanism through an orbital with some s-character, is very small and obscured already by small exchange effects. However, as shown by the good agreement between experimental and calculated NMR shifts as well as indirectly by the ESI-MS evidence presented in the synthesis section, the resting state of the compounds is rather long-lived and probably the structure as it is adopted in the solid state. These observations and the result of the calculations are best accounted for by assuming a rotation of the olefin around the $Ag-(C{=}C)_{bondcentroid}$ vector during which Ag−C coupling is destroyed but the olefin still remains coordinated to the silver atoms. Figure 9 on the right provides an alternative channel through which dynamics that cancels coupling to silver may occur without disconnecting from the silver ion.

To prevent the dynamics, low-temperature NMR measurements of **3** were performed. However, even with fairly diluted samples, the compounds started to crystallize at approximately +5 °C. Above this temperature, the system was still too flexible, whereas below 0 °C the signals immediately became very broad and weak. Therefore it was not possible to obtain low-temperature NMR data nor to observe coalescence or to determine the $^{1}J_{AgC}$ coupling constant.

Vibrational Spectroscopy. The IR and Raman spectra of **3** and **4**, especially the sections between 400 and 1400 cm^{-1} shown in Figure 10, exhibit the typical bands of the perfluorinated alkoxy aluminate anion in the range between 286 and 1353 cm^{-1}. However, due to very similar structural elements, especially of the perfluorinated ^{t}BuO groups, an exact distinction and assignment to cation and anion bands is almost impossible. Therefore all OR^F bands have been assigned to the anion. The assignment of the anion bands may easily be done by comparison to other salts of this anion such as $[H(OEt_2)_2][Al(OC(CF_3)_3)_4]$[13] and to the calculated vibrational frequencies. Since this was already done several times before,[13] the assignment of

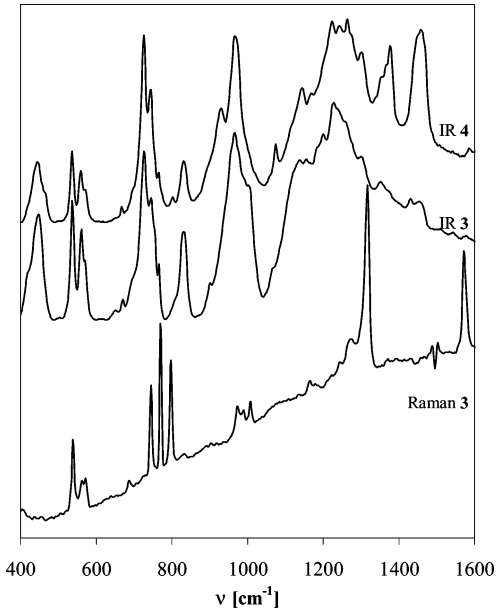

Figure 10. Sections of the IR and Raman spectra of **3** and **4**. IR spectra (top) were recorded in Nujol mulls between CsI plates; Raman sample (bottom) in a flame-sealed capillary.

the anion bands is not discussed in detail (a table with all anion bands of **3** and **4** including comparison to other anions and calculations is deposited in the Supporting Information). Compared to the calculated frequencies and the $[H(OEt_2)_2]^+$ salt, the positions of the anion bands remain almost unchanged. This indicates that there is no strong coordination of the anion as, for example, occurs with the naked Li^+ or Ag^+ cation.[12]

After elimination of the anion bands the remaining IR and Raman bands were assigned to the cations of **3** and **4** (Table 5) and show a generally good correspondence with the calculated frequencies. Most of the bands refer to vibrations of the trigonal bipyramidal core, especially those between 400 and 1300 cm^{-1}, with the exception of the CH_2 bending modes of the coordinated ethene between 1002 and 1007 cm^{-1}. C═C and C−H stretching modes of the alkene ligands can be observed in the Raman spectra between 1300 and 3100 cm^{-1}. For L = C_2H_4 these bands are 1316 (100), 1572, (44), 3009 (59), and 3092 (11) cm^{-1}. Compared to the respective Raman bands of $Ag(C_2H_4)_3^+$ at 1326, 1585, 3010, and 3096 cm^{-1},[43] the ligand is slightly stronger bound, indicated by a red shift of the CH_2 bending and the C═C stretching modes ($\Delta\nu$ = 10 and 13 cm^{-1}, cf. gaseous C_2H_4: 1342 and 1623 cm^{-1}[44]). However, this also implies that the bonds to the alkoxide groups are rather weak and, therefore, this cation is probably the closest approximation to a free $Ag(C_2H_4)^+$ moiety. For L = *i*-C_4H_8, the situation is slightly more difficult: Bands of the ligand were observed at 1378 (17), 1393 (24), 1407 (20), 1428 (17), 1586 (27), 2927 (39), 2993 (75), and 3057 (5) cm^{-1}. Among these bands the most important signal at 1586 cm^{-1} can be assigned to the C═C stretching mode. All other bands originate from C−H stretching or bending modes.

Solid-State Structures. The solid-state structures of **3** and **4** were determined, confirming the spectroscopic data and showing an ionic lattice of $[(AgL)_3(OR^F)_2]^+$ (L = C_2H_4, C_4H_8) and $[Al(OR^F)_4]^-$. The molecular structure of one formula unit of **3** is shown in Figure 11.

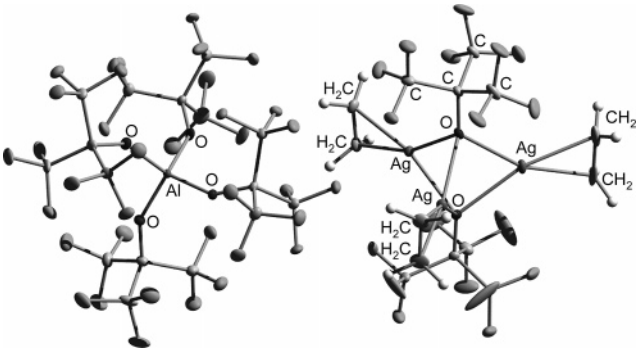

Figure 11. Section of the solid-state structure of **3**. Thermal ellipsoids were drawn at the 25% probability level; one cocrystallized CH_2Cl_2 molecule was omitted for clarity. Hydrogen atoms of the ligand were added and isotropically refined. Bond lengths of the anionic part: Al−O 171.3(5) to 173.5(5) pm (av 172.9 pm); C−O 134.0(8) to 137.9(8) pm (av 135.8 pm); C−C 148.2(17) to 159.8(10) pm (av 155.8 pm); C−F 129.1(9) to 138.3(16) pm (av 133.8 pm). Structural parameters for the cationic part are given in Table 6.

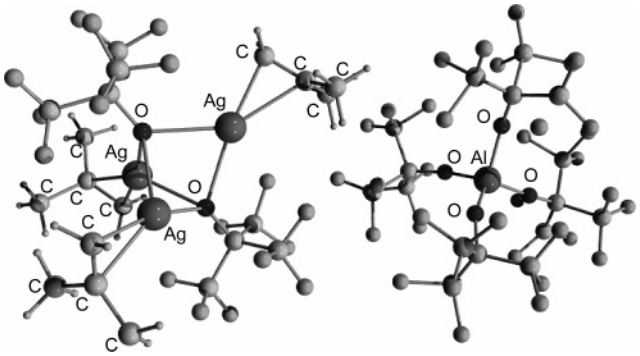

Figure 12. Ball-and-stick model of the solid-state structure of **4**.

Scheme 1. Set of Reactions Assessed for the Formation and Decomposition of $Ag_2(OR)_2^+$ [a]

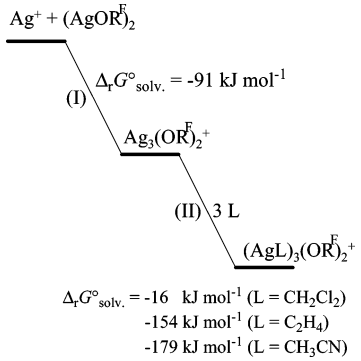

[a] DFT (BP86/TZVPP)-calculated Gibbs energies $\Delta_rG°$ in CH_2Cl_2 solution (COSMO solvation model).

The solid-state structure of **4** was also determined by X-ray crystallography. The NMR data could be confirmed as well as the existence of an ionic lattice of $[(AgC_4H_8)_3(OR^F)_2]^+$ and $[Al(OR^F)_4]^-$; however, the quality of the data does not allow for extensive discussions and the structure is mainly seen as additional evidence for the nature of **4** being a salt of the trigonal bipyramidal $[Ag_3X_2]^+$ (X = OR^F) cation (Figure 12). For the anions in **3** and **4** typical structural parameters as those reported earlier[12,45] were found.

(42) Hesse, M.; Meier, H.; Zeeh, B. *Spektroskopische Methoden in der Organischen Chemie*, 7th ed.; Thieme: Stuttgart, 2005; p 456.
(43) Reisinger, A.; Breher, F.; Deubel, D. V.; Krossing, I. Publication in progress.
(44) National Institute of Standards and Technology; http://www.nist.gov.
(45) Gonsior, M.; Krossing, I.; Müller, L.; Raabe, I.; Jansen, M.; Van Wüllen, L. *Chem.−Eur. J.* **2002**, *8*, 4475−4492.

Table 6. Average Distances for Selected Bonds of the Cationic Parts of 3 in Comparison with $Ag_3(NCO)_2(dppm)_3^+$ [26] and DFT (BP86/TZVPP)-Calculated Values (all data given in pm)

	calculation **3**	X-ray $[(AgC_2H_4)_3(OR^F)_2]^+$ (**3**)	X-ray $[Ag_3(NCO)_2(dppm)_3]^+$ [26]
d(Ag−Ag)	334.8	331.3 (326.12(5)−335.13(4))	330.2 (319.43(6)−346.90 (6))
d(Ag−O,N)	235.1	233.5 (229.7(5)−235.3(5))	249.1 (235.5(4)−258.6(5))
d(Ag−C)	225.7	228.9 (225.3(7)−231.0(8))	
d(C═C)	137.4	135.1 (133.3(13)−136.8(15))	

Table 7. Summary of Crystallographic Data Collection for 1a, 1b, 2a, 2b, 3, and 4

	1a	**1b**	**2a**	**2b**	**3**	**4**
formula	$C_{12}H_{16}F_9LiO_3$	C_4F_9LiO	$C_{4.5}HF_9OClAg$	C_4F_9OAg	$C_{31}H_8F_{54}O_6Cl_2Ag_3Al$	$C_{37}H_{26}F_{54}O_6Cl_2Ag_3Al$
T [K]	100(2)	100(2)	100(2)	100(2)	100(2)	100(2)
cryst syst	monoclinic	monoclinic	tetragonal	triclinic	orthorhombic	monoclinic
space group	$P2_1/n$	$P2_1/c$	$I4_1/acd$	$P\bar{1}$	$Pca2_1$	$P2_1$
a [pm]	894.98(18)	1651.9(3)	1937.3(3)	681.08(14)	2801.5(6)	1197.8(2)
b [pm]	1029.5(2)	1105.8(2)	1937.3(3)	1012.2(2)	1966.7(4)	1634.0(3)
c [pm]	1759.8(4)	1679.4(3)	1063.2(2)	1092.0(2)	1995.7(4)	3169.6(6)
α [deg]	90	90	90	85.76(3)	90	90
β [deg]	96.52(3)	104.33(3)	90	89.62(3)	90	90.19(3)
γ [deg]	90	90	90	88.93(3)	90	90
V [nm^3]	1.6109(6)	2.9722(10)	3.9901(11)	7.507(3)	11.00(1)	6.20(1)
Z	4	16	8	4	8	4
ρ(calcd) [g/cm^3]	1.592	2.163	2.559	3.034	2.332	2.157
absorp coeff [mm^{-1}]	0.177	0.293	2.400	2.825	1.397	1.243
F(000)	784	1856	2880	640	7376	3880
cryst size [mm^3]	0.2 × 0.2 × 0.3	0.5 × 0.5 × 0.1	0.2 × 0.2 × 0.4	0.5 × 0.3 × 0.2	0.25 × 0.4 × 0.35	0.15 × 0.3 × 0.25
θ range for data collection [deg]	3.66 to 24.71	1.27−25.00	2.97−27.5	3.52−30.62	3.31−30.02	3.32−24.71
index ranges	$-10 \le h \le 10$, $-12 \le k \le 12$, $-20 \le l \le 20$	$-19 \le h \le 19$, $-13 \le k \le 12$, $-19 \le l \le 19$	$-17 \le h \le 25$, $-24 \le k \le 20$, $-13 \le l \le 13$	$-9 \le h \le 9$, $-14 \le k \le 13$, $-14 \le l \le 15$	$-38 \le h \le 39$, $-27 \le k \le 27$, $-28 \le l \le 28$	$-14 \le h \le 14$, $-19 \le k \le 19$, $-37 \le l \le 37$
no. of reflns collected	41 237	29 407	6925	19 041	256 328	140 086
no. of indep reflns	2725	5199	1150	4000	31 498	21 023
no. of data/restraints/params	2725/0/236	5199/0/541	1150/23/138	4000/0/271	31498/1/1748	21 023/405/1856
goodness-of-fit on F^2	1.147	1.157	1.051	1.133	1.114	1.072
final *R* indices [$I > 2\sigma(I)$]	R1 = 0.0303, wR2 = 0.0679	R1 = 0.0792, wR2 = 0.1074	R1 = 0.0597, wR2 = 0.1378	R1 = 0.0352, wR2 = 0.0448	R1 = 0.0511, wR2 = 0.0943	R1 = 0.0951, wR2 = 0.2238
R indices (all data)	R1 = 0.0431, wR2 = 0.0770	R1 = 0.1774 wR2 = 0.1367	R1 = 0.1024, wR2 = 0.1664	R1 = 0.0563, wR2 = 0.0493	R1 = 0.0894, wR2 = 0.1158	R1 = 0.1350, wR2 = 0.2552
largest peak and hole [e $Å^{-3}$]	0.270; −0.222	0.672; −0.494	1.137; −0.778	0.714; −0.787	1.815; −1.260	2.404; −1.154

Trigonal bipyramidal cage cations have already been observed as part of the chelate-donor-stabilized $Ag_3X_2^+$ cation (X = Cl, Br, I, NCO, RC_2).[26−28] Unlike the strong diphosphine donors used in the latter compounds, every Ag atom in **3** and **4** is η^2 coordinated by only one alkene ligand L. In Table 6 selected bond distances of the cationic parts of **3** are listed and compared to calculated values.

As shown in Table 6, the Ag−C distances range from 225.3(7) to 231.0(8) pm (228.9 pm av). This means they are significantly shorter than in $[Ag(C_2H_4)_3]^+$ (239.6 pm av).[15,43] Thus, the Ag−C distances are best compared with calculated distances of an isolated $Ag(C_2H_4)^+$ moiety (230.6 pm, DFT calculation BP86/TZVPP). The C═C bond distances of 135.1 pm av (133.3(13)−136.8(15)) are elongated by 1.7/3.8 pm compared to free gaseous/solid ethene (133.4[40,46]/131.3 pm[47]), whereas the calculated bond distances of 137.4 pm are elongated by 3.1 pm compared to calculated ethene (134.3 pm).

However, the exact determination of light atom bond distances in proximity to heavy atoms such as Ag is difficult, and vibrational spectroscopy may be more accurate to detect such changes. Recently we have shown that the bond elongation Δ*d* and the decrease of the C═C stretching mode Δ*ν* in metal ethene complexes show a linear dependency with a proportionality constant $m = 29.1$ (pm cm)$^{-1}$.[43] With an experimental Δ*ν* of 51 cm^{-1} for **3** one would expect Δ*d* = 1.75 pm. Thus it appears that the C═C distance in **3** should be best compared to that in gaseous ethene, which also gives Δ*d* of 1.7 pm. However, the predicted elongation and, therefore, the Ag−C_2H_4 interaction is far overestimated by the calculations (Δ*d* = 3.1 pm; Δ*ν* = 101 cm^{-1}). Furthermore, this conclusion implies also that the C═C distances of free solid ethene must be too short.[47]

Interestingly our experimental Δ*d* from X-ray crystallography has sensible values with respect to Δ*ν*, which, mainly due to libration even at 100 K, was not the case for other Ag−ethene complexes.[48] This indicates that the C_2H_4 ligands are restricted in their thermal movement. This assumption is supported by 22 weak H···F contacts between the cation and the anion that range from 2.53 to 2.90 Å (av 2.74 Å; sum of van der Waals radii: 2.90 Å[40]) and tie the ethene ligand to its place.

The Ag−Ag distances (326.12(5)−335.13(4) pm; 331.3 pm av) are only slightly shorter than the sum of their van der Waals radii (340 pm).[40] Nevertheless, these distances are in very good agreement with other $Ag_3X_2(dppm)_3^+$ moieties, e.g., X = NCO (330.2 pm), Cl (338.5 pm), Br (333.9 pm), I (322.4 pm).[26] Only one exception exists: the silver alkynyl complex $[Ag_3(CCPh)_2$-

(46) Duncan, J. L.; Wright, I. J.; Van Lerberghe, D. *J. Mol. Spectrosc.* **1972**, *42*, 463−477. Van Lerberghe, D.; Wright, I. J.; Duncan, J. L. *J. Mol. Spectrosc.* **1972**, *42*, 251−273. Sutton, L. E. *Tables of Interatomic Distances and Configuration in Molecules and Ions*; Chemical Society: London, 1958.

(47) Van Nes, G. J. H.; Vos, A. *Acta Crystallogr., Sect. B: Struct. Sci.* **1979**, *35*, 2593−2601.

(48) Dias, H. V. R.; Wang, X. *J. Chem. Soc., Dalton Trans.* **2005**, 2985−2987. Dias, H. V. R.; Wang, Z. *Inorg. Chem.* **2000**, *39*, 3724−3727.

$(dppm)_3]^+$, with a shorter distance of 292.5 pm.[28] The Ag−O distances in **3** (229.7(5)−235.3(5) pm; 233.5 pm av) are similar to the sum of the ionic radii of Ag^+ and O^{2-} (236 pm[40]). These observations lead to the conclusion that possible Ag−Ag interactions are supposed to be very weak. Therefore the Ag_3X_2 moieties may be viewed to consist of three $[Ag(C_2H_4)]^+$ cations and two $[OC(CF_3)_3]^-$ anions that are held together mainly by electrostatic interactions, although they formally may also be described as closo clusters (12 VE).

Structure of $[Ag_3OR^F_2]^+$. From the experiment it is clear that the presence of a soft donor such as C_2H_4, C_4H_8, or CH_3CN is crucial for the successful synthesis of the cage cation. By contrast, with CH_2Cl_2 as a donor the reaction does not work. To find a reason for this completely different behavior, we assessed the following set of (partly hypothetical) reactions (Scheme 1).

The first step (I) describes the formation of the trinuclear $[Ag_3(OR^F)_2]^+$ framework and does not depend on the ligand L. The calculated Gibbs energy for this step is −91 kJ mol^{-1}. It appears that the $[Ag_3(OR^F)_2]^+$ framework has to be additionally stabilized by suitable donors such as C_2H_4, C_4H_8, or CH_3CN, which further stabilize the cage cation by −154 to −179 kJ mol^{-1} (step II). In contrast, complexation by CH_2Cl_2 liberates only −16 kJ mol^{-1} (Scheme 1), indicating a considerably less stable complex with CH_2Cl_2 as a ligand. Therefore it is reasonable that the hypothetical $[(AgCH_2Cl_2)_3(OR^F)_2]^+$ cage cation preferentially dissociates—as observed in our experiments—with formation of the hemisolvate **2a**.

Conclusion

The complete structural characterization of $LiOR^F$ (**1**) and facile preparation and complete experimental and computational characterization of $AgOR^F$ (**2**) were achieved. The first Ag alkoxide, **2**, may be an attractive reagent for synthesis including new mixed alkoxyaluminate salts by reaction with the Lewis acid $Al(OR^F)_3$.[49] This route should enable the synthesis of Ag salts that could not be synthesized via metathesis reaction of the corresponding Li salt; that is, $SbCl_5$ reacted with LiOR only to give $Li[SbCl_2(OR^F)_4]$ but not further. $AgOR^F$ might overcome this deficiency (cf. the reaction of $AgOTeF_5$ with MCl_5 (M = Sb, Nb)).[50] Apart from being a versatile synthon for anion synthesis, we currently test **2** as a precursor for CVD processes. It could be shown that **2** enables novel organometallic chemistry such as the successful synthesis of the trinuclear cage cations in **3** and **4**. These complexes are structurally closely related to a series of trinuclear group 10 and 11 cage compounds;[18−33] however, **3** and **4** are the first $[M_3X_2]$ cage compounds that could be stabilized without chelating diphosphine ligands.

Experimental Section

General Procedures. Due to the air and moisture sensitivity of most materials, all manipulations were undertaken using standard vacuum and Schlenk techniques as well as a glovebox with a nitrogen atmosphere (H_2O and O_2 < 1 ppm). All solvents were dried by conventional drying agents and distilled afterward. NMR spectra were recorded in CD_2Cl_2 at room temperature on a Bruker Avance 400 spectrometer. Data are given in ppm relative to the internal residual solvent signals (^1H, ^{13}C) or external aqueous $AlCl_3$ (^{27}Al) and $CFCl_3$ (^{19}F). IR spectra were obtained in Nujol mulls between CsI plates on a Bruker Vertex 70 IR spectrometer; Raman spectra were recorded on a Bruker RAM II Raman module using a highly sensitive Ge detector. The mass spectrum was recorded on a Finnigan SSQ 710C mass spectrometer with an electrospray ion source.

Preparation of $LiOR^F$ (1). Lithium hydride (0.35 g, 43.7 mmol) was weighed into a 250 mL round-bottom flask with a glass valve and suspended in Et_2O (∼70 mL). Nonafluoro-*tert*-butanol (6.1 mL, 43.8 mmol) was added dropwise over 30 min to the white suspension. After H_2 formation had finished, the reaction mixture was stirred for 1 h at room temperature and refluxed for 2 h afterward. Subsequently the solvent was removed and the resulting pure white precipitate of **1** was dried *in vacuo*. Yield: 10.47 g, 43.3 mmol (98.9%). Part of the resulting white powder was recrystallized from hot (90 °C) *o*-difluorobenzene to give very thin crystalline plates of tetrameric **1**. ^7Li NMR (156 MHz, CD_2Cl_2): δ −2.81 (s). $^{13}C[^1H]$ NMR (100 MHz, CD_2Cl_2): δ 83.1 (dez, $^2J_{CF}$ = 28.1 Hz), 124.2 (q, $^1J_{CF}$ = 292.4 Hz). ^{19}F NMR (376 MHz, CD_2Cl_2): δ −77.42 (s). IR (CsI plates, Nujol): ν 408 (w), 459 (ms), 520 (mw), 535 (m), 571 (w), 691 (w), 726 (s), 766 (m), 972 (vs), 1110 (m), 1176 (s), 1200 (s), 1240 (vs), 1279 (s) cm^{-1}. Raman: ν 116 (5), 167 (1), 220 (13), 309 (21), 329 (28), 344 (34), 419 (6), 458 (4), 537 (21), 571 (10), 690 (5), 769 (100), 976 (1), 1113 (4), 1168 (7), 1240 (5), 1282 (8), 1320 (17) cm^{-1}.

Preparation of $AgOR^F$ (2). $LiOC(CF_3)_3$ (1.35 g, 5.136 mmol) and $AgBF_4$ (1.00 g, 5.137 mmol) were mixed in the glovebox and weighed into one side of a two-bulb frit plate flask with a glass stem that was closed with two greaseless Young valves and wrapped in aluminum foil to exlude daylight. The mixture was suspended in CH_2Cl_2 (∼30 mL) and stirred overnight at room temperature. The next day the solution was filtered and all solvent removed. Afterward the white product was dried quickly in vacuo, since drying over a longer period caused decomposition. Large amounts of single crystals of **2a** were obtained by recrystallization from CH_2Cl_2 at −40 °C; small crystals of **2b** by sublimation at 130 °C and 10^{-2} mbar. Isolated yield: 1.71 g, 4.437 mmol (86%). ^1H NMR (400 MHz, CD_2Cl_2): δ 5.30 (s). $^{13}C[^1H]$ NMR (100 MHz, CD_2Cl_2): δ 82.0 (dez, $^2J_{CF}$ = 26.9 Hz), 122.9 (q, $^1J_{CF}$ = 293.3 Hz). ^{19}F NMR (376 MHz, CD_2Cl_2): δ −75.94 (s). IR (CsI plates, Nujol): ν 405 (w), 435 (vw), 493 (mw), 510 (vw), 537 (m), 573 (w), 726 (ms), 767 (m), 801 (mw), 966 (vs), 1135 (m), 1163 (ms), 1240 (vs), 1261 (s), 1303 (ms), 1377 (ms), 1460 (s), 2726 (w), 2850 (vs), 2900 (vs), 2947 (vs) cm^{-1}. Raman: ν 108 (14), 168 (5), 220 (7), 300 (16), 329 (35), 361 (9), 539 (19), 573 (5), 680 (5), 726 (4), 770 (100), 806 (4), 984 (9), 1008 (9), 1114 (7), 1165 (9), 1240 (4), 1262 (9), 1290 (9), 1315 (14), 2757 (32), 2845 (4), 2909 (29), 2937 (38) cm^{-1}.

Preparation of $[(Ag(L))_3(OR^F)_2][Al(OR^F)_4]$: General Procedure. $AgOR^F$ (0.256 g, 0.744 mmol) and $Ag[Al(OR^F)_4]$ (0.4 g, 0.372 mmol) were mixed in a glovebox and weighed into one side of a two-bulb frit plate flask with a glass stem that was closed with two greaseless Young valves. Both compounds were dissolved in CH_2Cl_2 (∼20 mL) to give a clear, slightly brownish solution. The flask was frozen using liquid nitrogen, and L (1.302 mmol; C_2H_4: 0.037 g; *i*-C_4H_8: 0.074 g) was condensed directly onto the mixture. Subsequently it was allowed to reach room temperature, whereby a white precipitate of the product formed. The precipitate was filtered off and extracted, leading to a CH_2Cl_2 solution. After slowly cooling the solution to 5 °C, crystals grew in large numbers directly from this solution. Since both compounds are decomposed upon evacuation, the yield could not be determined. However, it appears that the transformation is essentially quantitative.

L = C_2H_4 (3). MS: *m/z* [fragment, relative intensity] 493 [$C_6H_3ONF_9Ag_2^+$, 0.1%], 534 [$C_8H_6ON_2F_9Ag_2^+$, 0.2%], 833 [0.3%], 836 [$C_{10}H_3O_2NF_{18}Ag_3^+$, 0.3%], 877 [$C_{12}H_6O_2N_2F_{18}Ag_3^+$, 100%]. ^1H NMR (400 MHz, CD_2Cl_2): δ 5.54 (s). $^{13}C[^1H]$ NMR (100 MHz, CD_2Cl_2): δ 112.2 (s), 122.0 (q, $^1J_{CF}$ = 292.7 Hz), 122.9 (q, $^1J_{CF}$ =

(49) Krossing, I.; Gonsior, M.; Müller, L. 2004-EP12220 2005054254, 20041028, 2005.

(50) Van Seggen, D. M.; Hurlburt, P. K.; Anderson, O. P.; Strauss, S. H. *Inorg. Chem.* **1995**, *34*, 3453−3464.

292.1 Hz). ^{19}F NMR (376 MHz, CD_2Cl_2): δ −75.74 (s, 36F), −75.38 (s, 18F). ^{27}Al NMR (104 MHz, CD_2Cl_2): δ 31.92 (s). IR (CsI plates, Nujol): ν 380 (mw), 448 (ms), 537 (m), 561 (m), 571 (mw), 651 (w), 671 (w), 726 (ms), 744 (m), 766 (mw), 832 (m), 902 (w), 966 (s), 1002 (m), 1139 (ms), 1156 (ms), 1200 (s), 1228 (vs), 1300 (ms), 1352 (m), 1431 (w), 1454 (mw), 1542 (w), 1578 (vw), 2852 (ms), 2921 (m), 2954 (ms), 3009 (m), 3118 (w) cm^{-1}. Raman: ν 168 (4), 233 (20), 293 (55), 324 (69), 367 (24), 405 (10), 538 (40), 562 (16), 572 (16), 687 (5), 746 (49) 770 (80), 797 (58), 834 (4), 903 (3), 975 (15), 989 (11), 1007 (14), 1165 (6), 1222 (4), 1244 (10), 1274 (21), 1316 (100), 1572 (44), 2757 (18), 2909 (11), 2937 (16), 3009 (59), 3092 (11) cm^{-1}.

L = *i*-C_4H_8 (4). ^{1}H NMR (400 MHz, CD_2Cl_2): δ 2.09 (s, 6H), 4,89 (s, 2H). ^{13}C[^{1}H] NMR (100 MHz, CD_2Cl_2): δ 26.1 (s), 27.3 (s), 79.7 (b), 82.0 (b), 93.8 (s), 95.4 (s), 122.0 (q, $^1J_{CF}$ = 293.2 Hz), 122.8 (q, $^1J_{CF}$ = 292.9 Hz). ^{19}F NMR (376 MHz, CD_2Cl_2): δ −75.85 (s, 18F), −75.74 (s, 36F). ^{27}Al NMR (104 MHz, CD_2Cl_2): δ 31.91 (s). IR (CsI plates, Nujol): ν 446 (m), 537 (m), 560 (mw), 669 (w), 726 (s), 744 (ms), 765 (w), 801 (w), 831 (mw), 930 (m), 966 (s), 1075 (mw), 1144 (m), 1169 (mw), 1224 (s), 1243 (s), 1263 (s), 1301 (ms), 1376 (ms), 1459 (s), 1586 (w) 2726 (w), 2845 (s), 2901 (s), 2947 (s), 3177 (w) cm^{-1}. Raman: ν 171 (3), 234 (6), 288 (80), 324 (27), 370 (5), 431 (6), 468 (16), 540 (14), 563 (5), 573 (6), 707 (100), 747 (37) 770 (36), 801 (44), 934 (14), 976 (2), 1004 (5), 1061 (11), 1159 (6), 1245 (3), 1277 (8), 1301 (7), 1378 (17), 1393 (24), 1407 (20), 1428 (17), 1469 (6), 1586 (27), 2745 (4), 2837 (3), 2927 (39), 2993 (75), 3057 (5) cm^{-1}.

X-ray Structure Determination. Crystals suitable for X-ray diffraction experiments of compounds **1** to **4** were obtained as described above. Data were collected on a Bruker Kappa Apex II diffractometer using Mo Kα radiation (0.71073 Å) at T = 100 K. Single crystals were mounted in perfluoro ether oil using cryoloops (purchased from Hampton Research) and brought into the cold stream of a low-temperature device afterward so that the oil solidified.

Unit cell parameters were calculated from a least-squares refinement of the setting angles of 5000 reflections collected. The space groups were identified as $P2_1/n$ (**1a**), $P2_1/c$ (**1b**), $I4_1/acd$ (**2a**), $P\bar{1}$ (**2b**), $Pca2_1$ (**3**), and $P2_1$ (**4**). All structures were solved with direct (**1a**, **1b**, **2a**, **3**, **4**) or Patterson methods (**2b**) in SHELXS,[51] and successive interpretation of the difference Fourier maps was done using SHELXL-97. Refinement against F^2 was carried out with SHELXL-97. All non-hydrogen atoms were included anisotropically into the refinement; all hydrogen atoms were included isotropically at the calculated positions based on a riding model. Due to the disorder of the perfluorinated ^{t}Bu group in **2**, SADI commands were employed to restrain the respective bonds. The solid-state structure of **3** was refined as a racemic twin with a BASF value of 0.50514. **4** was refined as a twin with an inverted *b*-axis using the TWIN 1 0 0 0 0−1 0 0 0 1 command and a BASF value of 0.67041. An additional racemic twin could not be found; the absolute structure (Flack) parameter resided at 0.00(15). Due to the poor quality of the crystals, the anionic parts have been restrained with SADI and DFIX as well as ISOR commands. However, the cation in **4** is well behaved, and we therefore leave the structure in the paper mainly using it as additional proof for the nature of **4**. Yet, the structure of **4** is treated as preliminary and, as suggested by one of the referees, not deposited with the CCDC. Relevant data concerning crystallography, data collection, and refinement are compiled in Table 7. Crystallographic data excluding structure factors have been deposited with the Cambridge Crystallographic Data Centre as supplementary publication nos. 609257 (**1a**), 609258 (**1b**), 609259 (**2a**), 299939 (**2b**), and 609260 (**3**). Copies of the data can be obtained free of charge on application to CCDC, 12 Union Road, Cambridge CB21EZ, UK (fax: (+44)-1223-336-033; e-mail: deposit@ccdc.cam.ac.uk).

Computational Details. All quantum chemical calculations were carried out with the TURBOMOLE program package.[52] The geometries of all compounds were optimized in the highest possible point group symmetry by DFT calculations using the BP86[53] functional and SV(P) or TZVPP[54] basis sets. Vibrational frequencies were calculated at the BP86/SV(P) level and used to verify the nature of the obtained minima.[55] The calculated enthalpies were also corrected for the influences of the Gibbs energy at 298 K (using FreeH as implemented in TURBOMOLE) as well as solvent effects (COSMO model, CH_2Cl_2 solvent with ϵ_r = 8.93).[56]

Acknowledgment. This work was supported by the DFG, the SNF, the Ecole Polytechnique Fédérale de Lausanne (EPFL), and the Universität Freiburg. We thank Dr. Rosario Scopelliti (Lausanne) for his help with the diffractometers and Dr. Alain Razaname (Lausanne) for recording the mass spectra.

Supporting Information Available: Simulation of IR spectra based on calculations of vibrational frequencies, IR spectra, tables of optimized atomic coordinates from density functional calculations, and full listings of crystallographic details: atomic coordinates, displacement parameters, and complete bond distances, angles, and torsion angles. This material is available free of charge via the Internet at http://pubs.acs.org.

OM061046P

(51) Sheldrick, G. *SHELX-software suite*; University of Göttingen: Germany.

(52) Ahlrichs, R.; Baer, M.; Häser, M.; Horn, H.; Koelmel, C. *Chem. Phys. Lett.* **1989**, *162*, 165−169. von Arnim, M.; Ahlrichs, R. J. *Chem. Phys.* **1999**, *111*, 9183−9190.

(53) Becke, A. D. *Phys. Rev. A: At., Mol., Opt. Phys.* **1988**, *38*, 3098−3100. Perdew, J. P.; Burke, K.; Wang, Y. *Phys. Rev. B: Condens. Matter* **1996**, *54*, 16533−16539.

(54) Eichkorn, K.; Weigend, F.; Treutler, O.; Ahlrichs, R. *Theor. Chem. Acc.* **1997**, *97*, 119−124.

(55) Deglmann, P.; Furche, F.; Ahlrichs, R. *Chem. Phys. Lett.* **2002**, *362*, 511−518.

(56) Klamt, A.; Schüürmann, G. *J. Chem. Soc., Perkin Trans. 2* **1993**, 799−805. Schäfer, A.; Klamt, A.; Sattel, D.; Lohrenz, J. C. W.; Eckert, F. *Phys. Chem. Chem. Phys.* **2000**, *2*, 2187−2193.